Broad histogram method: Extension and efficiency test

M. Kastner* and M. Promberger
Institut für Theoretische Physik, Universität Erlangen–Nürnberg, Staudtstrasse 7, 91058 Erlangen, Germany

J. D. Muñoz†
Departamento de Física, Universidad Nacional de Colombia, Bogotá D.C., Colombia
(Received 5 August 1999; revised manuscript received 25 January 2000)

Compared to standard histogram techniques, the broad histogram method allows us to increase the efficiency of Monte Carlo simulations by a tremendous amount. This gain of efficiency is achieved by measuring simulation averages of particular system observables (different from those used in standard histogram techniques), while the algorithm of the simulation can be left unchanged. In this paper, the broad histogram method is reformulated in a more mathematical and precise way. Furthermore, the method is extended to estimate the density of states as a function of more than one parameter. A quantitative investigation of the gain of efficiency of Monte Carlo simulations is performed. For the broad histogram method, we find a gain of efficiency which amounts to orders of magnitude in comparison to the standard histogram method.

PACS number(s): 02.70.Lq, 05.10.−a

I. INTRODUCTION

In performing a Monte Carlo simulation, one or several observables are chosen, for which a simulation average is recorded. A common choice for such an observable gives rise to a standard histogram as introduced by Salsburg *et al.* [1] and popularized by Swendsen and Ferrenberg [2]. The histogram allows for the estimation of the density of states Ω, from which a variety of physically interesting system properties can be computed. The broad histogram method (BHM) as recently suggested by Oliveira *et al.* [3] likewise enables an estimation of the density of states but leads to a considerable reduction of the computing time. This reduction is achieved by measuring simulation averages of particular (system) observables, different from those which yield a standard histogram, while the algorithm of the simulation can be left unchanged.

From the method presented in [3], the density of states Ω can be computed as a function of one variable, the energy E. In general, this does not enable the determination of the entire set of equations of state describing the behavior of the system. The entire set can be obtained from the density of states as a function of more than one parameter. To this very aim, an extension of the BHM is required. For the case of the standard Ising model, such an extension is shown to yield the density of states $\Omega(E,M)$ as a function of the energy E and the magnetization M.

If the standard histogram method is applied to magnetic systems, the number of microstates with energy E and magnetization M is counted during the course of simulation, i.e., every microstate yields *one* entry in an energy-magnetization histogram. From this histogram, the density of states $\Omega(E,M)$ can be computed (see Sec. II C).

In the BHM, each microstate of the Monte Carlo sample is exploited in a much more sophisticated way. For the particular realization of the method introduced in Sec. III, this means that in an extended histogram, which is defined as the simulation average of the so-called transition observable to be introduced below, the number of possible transitions is recorded from particular microstates (in the Monte Carlo sample) with energy E and magnetization M to ''neighboring'' microstates (not necessarily in the Monte Carlo sample) with energy $E \pm \Delta E$ and magnetization $M \pm \Delta M$, which can be reached from the particular microstates of the sample by applying single spin-flip operations. Again, from the simulation averages of the transition observables, the density of states can be computed (see Sec. II D).

The advantage of this method is that every microstate of the Monte Carlo sample is investigated much more extensively than by the standard histogram technique. Therefore, given a certain sample of microstates, the density of states can be calculated more accurately from simulation averages of the transition observable than by standard methods. Additionally, as it is the selection of microstates using pseudorandom numbers which is costly in computer time, the increase in computer time from such a more extensive exploration of the chosen microstates is absolutely negligible (at least in the case of the particular realization of the method introduced below). However, the effect on the data quality is significant and can amount to orders of magnitude. In the case of the examples studied in this paper, we find an efficiency gain of roughly two orders of magnitude. This efficiency gain can be expected to grow proportional to $L^{d/2}$, the square root of the volume of the system. It is this enormous gain of efficiency which should motivate the reader to focus on the underlying formalism, which is indeed simple to implement in a simulation, but is somewhat heavy to formalize.

In this paper we show that it is straightforward to extend BHM to more than one parameter. Quantitative investigations of the efficiency of this method in comparison to standard histogram methods are presented. Sections II A and II B aim to familiarize the reader with the language used throughout this paper and with some aspects of the Monte Carlo

*Corresponding author.
†Present address: ICA1 Universität Stuttgart, Pfaffenwaldring 27, 70569 Stuttgart, Germany.

procedure. In Sec. II C, the standard histogram technique is reviewed in the context of the calculation of the density of states. In the context of the BHM, the transition observable is introduced in Sec. II D. In Sec. II E, it is shown that this observable includes the one presented in [3] as a special case. The rest of the paper (Sec. III) is devoted to a comparison of the efficiency of computer simulations using the BHM in contrast to a standard histogram technique. This is done for the examples of $2d$- and $3d$-Ising systems, where we find a gain of efficiency of approximately 40 in the 32^2 Ising system and of approximately 250 in the 10^3 Ising system.

II. CALCULATING THE DENSITY OF STATES BY MONTE CARLO SIMULATION

A. Conventions and notation

In this paper, we use the language of discrete Ising systems with nearest-neighbor interactions on hypercubic lattices of linear size L in d spatial dimensions with Hamiltonian

$$\mathcal{H}(S) := -J\sum_{\langle i,j\rangle}\sigma_i\sigma_j - h\sum_i \sigma_i =: E(S) - hM(S), \quad S\in\Gamma_{L^d}, \tag{1}$$

where h denotes an external magnetic field. $E(S)$ is the interaction energy and $M(S)$ the magnetization of the particular microstate $S=\sigma_1,\sigma_2,\ldots,\sigma_i,\ldots,\sigma_{L^d}$ (=particular configuration of the spins σ_i, $i=1,2,\ldots,L^d$ on the L^d lattice) with $\sigma_i\in\{-1,+1\}$. The configuration space of the Ising system is denoted by Γ_{L^d}, and $\langle i,j\rangle$ indicates a summation over all pairs of nearest neighbors. The discreteness of the Ising systems gives rise to *minimal* energy and magnetization spacings, denoted by ΔE and ΔM, respectively. Summations over the interaction energy E (magnetization M) cover all energy (magnetization) values accessible for the system. In general, in order to simplify the notation, system size dependences are not stated explicitly. In what follows, we set the Ising coupling constant $J\equiv 1$ and Boltzmann's constant $k_B\equiv 1$.

B. Some remarks on Monte Carlo simulations

For a Monte Carlo simulation, a Markov process is set up on configuration space Γ_{L^d} with a certain problem-adapted stationary distribution $\hat{w}(S)$, which is assumed to depend only on the interaction energy E and the magnetization M of the microstate S, i.e., $\hat{w}(S)=w(E(S),M(S))$. [It is straightforward to extend the formalism introduced in the following sections to the case of a more general stationary distribution which, of course, may depend on system observables other than the interaction energy E and the magnetization M. The restricting assumption $\hat{w}(S)=w(E(S),M(S))$ is made only for the sake of notational simplicity]. From the Markov chain $\{S\}_{\mathcal{N}}$ of length $\mathcal{N}$ (which, at least in the limit of infinitely long samples, is distributed according to $\hat{w}$), the *simulation average* of an arbitrary function f: $\Gamma_{L^d}\to\mathbb{R}$ on configuration space can be obtained:

$$\langle f(S)\rangle_{\mathrm{sim},w}(\{S\}_{\mathcal{N}}) := \frac{1}{\mathcal{N}}\sum_{S\in\{S\}_{\mathcal{N}}} f(S) \overset{\mathcal{N}\to\infty}{\to} \sum_{S\in\Gamma_{L^d}} f(S)\hat{w}(S). \tag{2}$$

Of course, the simulation average depends on the stationary distribution and, unless the length of the Markov chain reaches infinity, on the particular sample $\{S\}_{\mathcal{N}}$.

C. The standard histogram method

The histogram $H_w(E,M;\{S\}_{\mathcal{N}})$, which is proportional to the number of microstates of the sample with interaction energy E and magnetization M, is given by the simulation average of the observable $\delta_{E(S),E}\delta_{M(S),M}$:

$$\begin{aligned} H_w(E,M;\{S\}_{\mathcal{N}}) &= \langle \delta_{E(S),E}\delta_{M(S),M}\rangle_{\mathrm{sim},w}(\{S\}_{\mathcal{N}}) \\ &= \frac{1}{\mathcal{N}}\sum_{S\in\{S\}_{\mathcal{N}}}\delta_{E(S),E}\delta_{M(S),M} \\ &\overset{\mathcal{N}\to\infty}{\to} \sum_{S\in\Gamma_{L^d}}\delta_{E(S),E}\delta_{M(S),M}w(E(S),M(S)) \\ &= \Omega(E,M)w(E,M), \end{aligned} \tag{3}$$

where δ denotes Kronecker's delta symbol. Since the underlying stationary distribution w is known (at least apart from an irrelevant factor), the density of states is obtained as

$$\begin{aligned} \Omega(E,M) &:= \sum_{S\in\Gamma_{L^d}}\delta_{E(S),E}\delta_{M(S),M} \\ &= \lim_{\mathcal{N}\to\infty} H_w(E,M;\{S\}_{\mathcal{N}})/w(E,M), \end{aligned} \tag{4}$$

or — more realistically for a computer simulation — at least an estimator for Ω is obtained by omitting the limiting procedure $\mathcal{N}\to\infty$.

D. The broad histogram method

In this section, it is shown that the density of states can be obtained from simulation averages of certain so-called transition observables defined below, which have the advantageous feature that they enable the estimation of the density of states in a much more efficient way than the standard histogram method does.

As a preliminary step, let us define the *microcanonical average* of a system observable $f(S)$:

$$\begin{aligned} \langle f(S)\rangle(E,M) &:= \lim_{\mathcal{N}\to\infty}\frac{\langle f(S)\,\delta_{E(S),E}\delta_{M(S),M}\rangle_{\mathrm{sim},w}(\{S\}_{\mathcal{N}})}{H_w(E,M;\{S\}_{\mathcal{N}})} \\ &= \frac{1}{\Omega(E,M)}\sum_{S\in\Gamma_{L^d}}\delta_{E(S),E}\delta_{M(S),M}f(S). \end{aligned} \tag{5}$$

Let $\mathcal{A}$ be a set of operators acting on configuration space Γ_{L^d},

$$\mathcal{A}\subseteq\{A: AS\in\Gamma_{L^d}\ \ \forall\ \ S\in\Gamma_{L^d}\}. \tag{6}$$

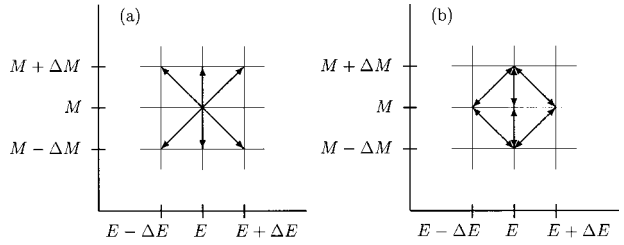

FIG. 1. (a) Visualization of the transition observables $N_{\mathcal{A}}^{i,j}$ for the case $i\in\{-1,0,1\}$ and $j\in\{-1,1\}$. Given a *particular* microstate S with interaction energy $E(S)=E$ and magnetization $M(S)=M$, $N_{\mathcal{A}}^{i,j}(S)$ gives the number of possibilities to reach any state $\tilde{S}$ with energy $E(\tilde{S})=E(S)+i\Delta E$ and magnetization $M(\tilde{S})=M(S)+j\Delta M$ by applying the operators $A\in\mathcal{A}$ to the microstate S. The microcanonical average of the transition observable $N_{\mathcal{A}}^{i,j}$ is proportional to the *total* number of possibilities for the event that, given *any* state S with energy $E(S)=E$ and magnetization $M(S)=M$, any other state $\tilde{S}$ with energy $E(\tilde{S})=E(S)+i\Delta E$ and magnetization $M(\tilde{S})=M(S)+j\Delta M$ is reached under the action of the operators $A\in\mathcal{A}$. (b) shows the ''transition paths'' corresponding to the various microcanonical expectation values contributing to the differences of the logarithm of the density of states $\Delta_M(\ln\Omega)$ at the point (E,M), as introduced in Sec. III.

The *transition observable* $N_{\mathcal{A}}^{i,j}(S)$ is defined as the number of operators $A\in\mathcal{A}$ acting on the particular microstate S which result in microstates $\tilde{S}$ with interaction energy $E(\tilde{S})=E(S)+i\Delta E$ and magnetization $M(\tilde{S})=M(S)+j\Delta M$:

$$N_{\mathcal{A}}^{i,j}(S):=\sum_{\tilde{S}\in\Gamma_{L^d}}\delta_{E(\tilde{S}),E(S)+i\Delta E}\delta_{M(\tilde{S}),M(S)+j\Delta M}\times\sum_{A\in\mathcal{A}}\delta_{AS,\tilde{S}},\quad i,j\in\mathbb{Z}. \tag{7}$$

(See Fig. 1 for an illustration of the thus defined observables.) Then, for any set $\mathcal{A}$ of operators which satisfies

$$0\neq\sum_{S\in\Gamma_{L^d}}\delta_{E(S),E}\delta_{M(S),M}N_{\mathcal{A}}^{i,j}(S)=\sum_{S\in\Gamma_{L^d}}\delta_{E(S),E+i\Delta E}\delta_{M(S),M+j\Delta M}N_{\mathcal{A}}^{-i,-j}(S), \tag{8}$$

the density of states $\Omega(E,M)$ can be calculated from the microcanonical averages (5) of the transition observables (7) to yield

$$\Omega(E,M)=\frac{\langle N_{\mathcal{A}}^{-i,-j}(S)\rangle(E+i\Delta E,M+j\Delta M)}{\langle N_{\mathcal{A}}^{i,j}(S)\rangle(E,M)}\times\Omega(E+i\Delta E,M+j\Delta M). \tag{9}$$

The following remarks are in order.

(i) Microreversibility as explained in Appendix A is a sufficient condition for the equality in Eq. (8). Apart from this condition, which is implemented easily, the set $\mathcal{A}$ of operators can be chosen arbitrarily.

(ii) In the density of states, a multiplicative constant is physically irrelevant. For that reason, Ω can be chosen arbitrarily for one particular value of (E,M). Then, the density of states of the remaining (E,M) values can be calculated from Eq. (9).

(iii)The efficiency of the BHM depends crucially on the particular choice of $\mathcal{A}$.

(iv) The BHM is neither restricted to the investigation of Ising systems (with bare next-neighbor interaction [4]) nor to the investigation of discrete systems [5]. Example: consider a discrete spin system with a Hamiltonian consisting of two interaction terms,

$$\mathcal{H}(S)=E_1(S)+E_2(S), \tag{10}$$

which depends on certain coupling constants, say, J_1 and J_2 (e.g., ferromagnetic coupling to next neighbors and antiferromagnetic coupling to next-nearest neighbors). The knowledge of the density of states as a function of E_1 and E_2,

$$\Omega(E_1,E_2):=\sum_{S\in\Gamma_{L^d}}\delta_{E_1(S),E_1}\delta_{E_2(S),E_2}, \tag{11}$$

enables the determination of the thermostatic properties of the system for *all* possible values of the ratio of the coupling constants by applying certain ''skew-summing'' techniques [6]. In complete analogy to the above, a set of transition observables can be defined which facilitates the determination of the thus defined density of states $\Omega(E_1,E_2)$.

(v) For a matrix $\mathbf{T}$ defined as

$$[\mathbf{T}]_{(E',M'),(E,M)}:=\frac{1}{|\mathcal{A}|}\left\langle N_{\mathcal{A}}^{\frac{E'-E}{\Delta E},\frac{M'-M}{\Delta M}}(S)\right\rangle(E,M), \tag{12}$$

where $|\mathcal{A}|$ is the cardinality of the set $\mathcal{A}$, it is easy to show the following: (a) $\mathbf{T}$ is a stochastic matrix, i.e.,

$$[\mathbf{T}]_{(E',M'),(E,M)}\geqslant 0\quad\forall\quad(E',M'),(E,M) \tag{13}$$

and

$$\sum_{(E',M')}[\mathbf{T}]_{(E',M'),(E,M)}=1; \tag{14}$$

(b) the density of states is the stationary state of $\mathbf{T}$:

$$\sum_{(E,M)}[\mathbf{T}]_{(E',M'),(E,M)}\Omega(E,M)=\Omega(E',M'). \tag{15}$$

Furthermore, if $\mathbf{T}$ is regular, i.e., if for all (E',M') and (E,M)

$$\exists n\in\mathbb{N}:[\mathbf{T}^m]_{(E',M'),(E,M)}>0,\quad\forall\quad m\geqslant n, \tag{16}$$

the stationary state of $\mathbf{T}$ is unique. Nevertheless, even if this condition is not fulfilled, the density of states can be computed piecewise on certain subsets of the total set of possible energy and magnetization values of the system. The thus produced ''fragments'' of the density of states are then connected to each other via (*a priori* unknown) multiplicative constants. Note that the stochastic matrix $\mathbf{T}$ defined above is closely related to the so-called transition matrix Monte Carlo method [7].

(vi) Note that the naming ''broad histogram method'' is extremely misleading since the heart of the BHM, the gen-

eration of simulation averages of the transition observable, has nothing to do with broad histograms, i.e., the shape of a histogram generated during the course of a Monte Carlo simulation.

E. The reduced transition observable

The results of Sec. II D can be simplified to those presented in [3], where no information on the magnetization of the system is regarded. Formally, this can be achieved by a summation over the magnetization M (or the index j, respectively) in some of the expressions of the preceding section. Then, however, only a determination of the *reduced density of states*

$$\tilde{\Omega}(E) := \sum_{M} \Omega(E,M) \tag{17}$$

is feasible, which does not entail the entire thermodynamic information of the system [in the sense that $\Omega(E,M)$ enables the calculation of thermal and magnetic equations of state in various ensembles, whereas $\tilde{\Omega}(E)$ just allows for the estimation of the thermal equation of state].

The *reduced microcanonical average* of a system observable $f(S)$ over the energy shell $E(S)=E$ is defined as

$$\langle f(S)\rangle(E) := \lim_{\mathcal{N}\to\infty} \frac{\langle f(S)\,\delta_{E(S),E}\rangle_{\mathrm{sim},w}(\{S\}_{\mathcal{N}})}{\sum_{M} H_w(E,M;\{S\}_{\mathcal{N}})}$$

$$= \frac{1}{\tilde{\Omega}(E)} \sum_{S\in\Gamma_{L^d}} \delta_{E(S),E}\, f(S). \tag{18}$$

We further define the *reduced transition observable*

$$\tilde{N}^i_{\mathcal{A}}(S) := \sum_{j\in\mathbb{Z}} N^{i,j}_{\mathcal{A}}(S)$$

$$= \sum_{\tilde{S}\in\Gamma_{L^d}} \delta_{E(\tilde{S}),E(S)+i\Delta E} \sum_{A\in\mathcal{A}} \delta_{AS,\tilde{S}}, \quad i\in\mathbb{Z}. \tag{19}$$

Then, for any set of operators $\mathcal{A}$ which satisfies

$$0 \neq \sum_{S\in\Gamma_{L^d}} \delta_{E(S),E} \tilde{N}^i_{\mathcal{A}}(S) = \sum_{S\in\Gamma_{L^d}} \delta_{E(S),E+i\Delta E} \tilde{N}^{-i}_{\mathcal{A}}(S), \tag{20}$$

the reduced density of states (17) can be calculated from the reduced microcanonical average (18) of the reduced transition observable (19):

$$\tilde{\Omega}(E+i\Delta E) = \frac{\langle \tilde{N}^i_{\mathcal{A}}(S)\rangle(E)}{\langle \tilde{N}^{-i}_{\mathcal{A}}(S)\rangle(E+i\Delta E)} \tilde{\Omega}(E). \tag{21}$$

Again, microreversibility (see Appendix A) is sufficient to ensure the equality in Eq. (20).

III. COMPARISON OF THE EFFICIENCY OF THE STANDARD HISTOGRAM METHOD AND THE BROAD HISTOGRAM METHOD

To demonstrate the advantages of the BHM, numerical results obtained from either the standard histogram method or the BHM are compared. The philosophy of the comparison is to use some simulation technique to generate *one* sample of microstates which is then evaluated according to *both* methods.

The simulations were performed for a $d=2$, $L=32$ and a $d=3$, $L=10$ Ising system. For the sake of completeness, the details of the computer simulations are given in Appendix C. The set $\mathcal{A}$ was chosen to consist of L^d operators, which are labeled by the subscript i and are defined by their action on a particular microstate S,

$$A_i : S=\sigma_1,\sigma_2,\ldots,\sigma_i,\ldots,\sigma_{L^d}$$

$$\mapsto \tilde{S}=\sigma_1,\sigma_2,\ldots,-\sigma_i,\ldots,\sigma_{L^d}, \tag{22}$$

i.e., the operator A_i flips the ith spin of the Ising lattice. Obviously, since $A_iA_iS=S$, the thus defined set of operators meets the condition (30) and is therefore microreversible. Note that the determination of the simulation average of the transition observable by use of this particular set of operators can be done very fast. In fact, the time needed for applying the L^d operators of the set $\mathcal{A}$ to a particular microstate is much shorter than the time needed to perform a lattice sweep. Simulation averages of $N^{i,j}_{\mathcal{A}}$ were recorded only for values of $i\in\{-1,0,1\}$ and $j\in\{-1,1\}$.

In order to emphasize the difference between the two methods, we compare ''discrete derivatives'' (i.e., ratios of differences) of the logarithm of the density of states as follows.

(i) For the case of the $d=2$ Ising model,

$$\Delta_E(\ln\tilde{\Omega}(E)) := \frac{1}{2\Delta E}[\ln\tilde{\Omega}(E+\Delta E) - \ln\tilde{\Omega}(E-\Delta E)] \tag{23}$$

$$= \frac{1}{2\Delta E} \ln\left[\frac{\langle \tilde{N}^1_{\mathcal{A}}(S)\rangle(E-\Delta E)\langle \tilde{N}^1_{\mathcal{A}}(S)\rangle(E)}{\langle \tilde{N}^{-1}_{\mathcal{A}}(S)\rangle(E+\Delta E)\langle \tilde{N}^{-1}_{\mathcal{A}}(S)\rangle(E)}\right]. \tag{24}$$

(ii) For the case of the $d=3$ Ising model,

$$\Delta_M(\ln\Omega(E,M)) := \frac{1}{2\Delta M}[\ln\Omega(E,M+\Delta M) - \ln\Omega(E,M-\Delta M)] \tag{25}$$

$$= \frac{1}{2\Delta M} \ln\left[\frac{\langle N^{1,1}_{\mathcal{A}}(S)\rangle(E,M-\Delta M)\langle N^{-1,1}_{\mathcal{A}}(S)\rangle(E+\Delta E,M)}{\langle N^{1,-1}_{\mathcal{A}}(S)\rangle(E,M+\Delta M)\langle N^{-1,-1}_{\mathcal{A}}(S)\rangle(E+\Delta E,M)}\right] \tag{26}$$

$$= \frac{1}{2\Delta M} \ln \left[\frac{\langle N_{\mathcal{A}}^{-1,1}(S) \rangle (E, M-\Delta M) \langle N_{\mathcal{A}}^{1,1}(S) \rangle (E-\Delta E, M)}{\langle N_{\mathcal{A}}^{-1,-1}(S) \rangle (E, M+\Delta M) \langle N_{\mathcal{A}}^{1,-1}(S) \rangle (E-\Delta E, M)} \right] \tag{27}$$

$$= \frac{1}{2\Delta M} \ln \left[\frac{\langle N_{\mathcal{A}}^{0,1}(S) \rangle (E, M-\Delta M) \langle N_{\mathcal{A}}^{0,1}(S) \rangle (E, M)}{\langle N_{\mathcal{A}}^{0,-1}(S) \rangle (E, M+\Delta M) \langle N_{\mathcal{A}}^{0,-1}(S) \rangle (E, M)} \right]. \tag{28}$$

Note that both ''discrete derivatives'' (23) and (25) are closely related to microcanonical equations of state (see [8] and Appendix B for details).

A. Example 1: The $d=2$, $L=32$ Ising lattice

In Fig. 2, the differences of the logarithm of the reduced density of states as emerging from the BHM (24) and the standard histogram method (4) are shown together with the exact result [9]. By use of a sample of 8×10^5 microstates, the BHM yields a result which, on the scale of the figure, can hardly be distinguished from the exact result, whereas the data obtained from the standard histogram method scatter strongly around the latter.

In Fig. 3, the results of the BHM (using *one* sample of $n=8\times10^5$ microstates) are compared to the results of the standard histogram method for several sample lengths (n, $5n$, $10n$, and $15n$) by plotting the deviation of the simulation data from the exact result. Even if the simulation time is chosen 15 times longer in the standard histogram method, the BHM still yields more accurate results.

Calculating the mean-square deviation of the simulation data from the exact result as a function of simulation time (Fig. 4), we notice that the accuracy of both methods is improved according to a power law [the corresponding exponents seem to be the same (approximately -1) in both methods]. At any given time, the BHM beats the standard histogram method in accuracy by a factor of roughly 40. The comparison of the data was done within a certain ''energy window'' which was chosen around the center of the histogram, i.e., the tails of the histogram have been discarded. Since the same sample is used in both evaluation techniques, the result of the comparison does not depend on the width of the ''energy window'' chosen for the evaluation of the χ^2 deviations.

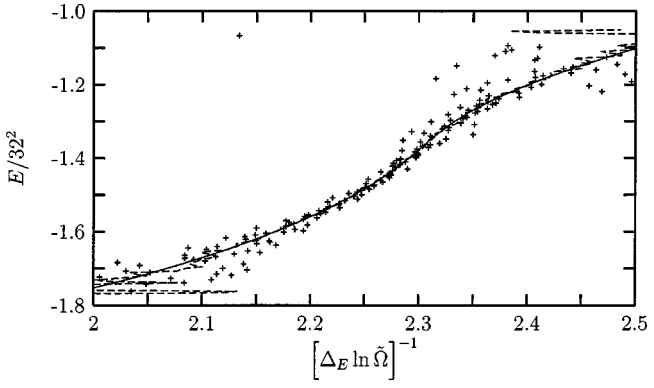

FIG. 2. Intensive energy as a function of $[\Delta_E(\ln \tilde{\Omega})]^{-1}$ of a 32^2 square Ising system. The solid line is the exact result, the dashed line corresponds to the BHM, and the points to the standard histogram method. An identical sample of 8×10^5 microstates was used to perform both evaluations. The energy is plotted against $[\Delta_E(\ln \tilde{\Omega})]^{-1}$ because of its correspondence to a thermal equation of state $E(T)$ (see Appendix B). The strong fluctuations in both the high-energy and the low-energy region of the figure are due to poor statistics in the tails of the histograms. In the central region, the difference between the dashed and the full line is smaller than the line thickness.

B. Example 2: The $d=3$, $L=10$ Ising lattice

From the Monte Carlo samples, we computed the differences of the logarithm of the density of states in the direction of the magnetization according to Eq. (4) in the case of the standard histogram method and according to Eqs. (26)–(28) in the case of the BHM [in fact, we computed the mean value of the three possibilities (26)–(28) of determining $\Delta_M(\ln \Omega)$].

In Figs. 5(a) and 5(b), $\Delta_M(\ln \Omega)$ is shown for $E/L^d = -0.924$. In Fig. 5(a), a sample of length 1×10^7 microstates is used for the evaluation of $\Delta_M(\ln \Omega)$ according to both methods, whereas in Fig. 5(b) the standard histogram method with a sample length of 5×10^7 microstates is compared to the BHM with a sample length 1×10^7 again. For a better visualization of the difference between the two meth-

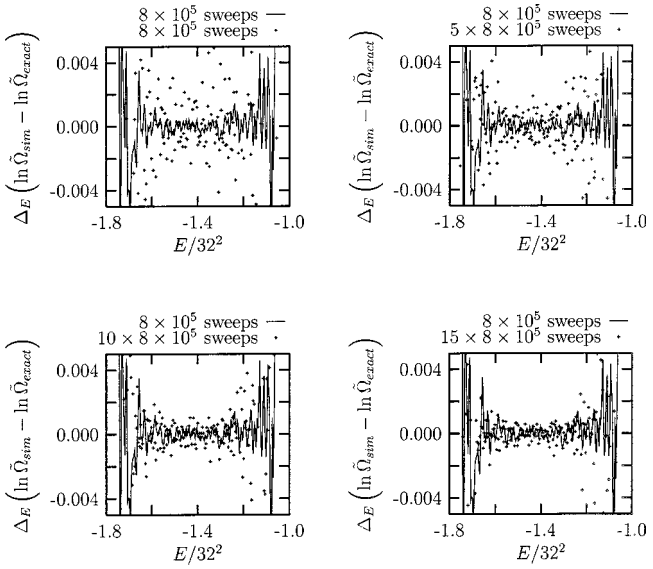

FIG. 3. In order to point out the differences between the BHM and the standard histogram method and in order to show that the used estimators are indeed unbiased, the data emerging from the Monte Carlo simulation of a 32^2 square Ising system are subtracted from the exact result [9]. The transition observable data (standard histogram data) are represented by solid lines (points).

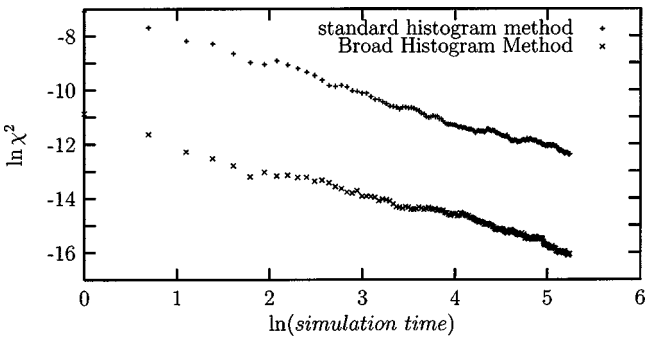

FIG. 4. In order to judge the quality of the two methods, the χ^2 deviation of the simulation results from the *exact* result is shown for a 32^2 square Ising system as a function of the simulation time (in units of 8×10^5 lattice sweeps).

ods, an odd polynomial $[f_{\rm fit}(M)=aM+bM^3+cM^5]$ was fitted to the BHM data. Subtraction of the data of Figs. 5(a) and 5(b) from this polynomial yields the plots shown in Figs. 5(c) and 5(d). In the figures, the BHM (standard histogram) data are represented by the solid lines (points). The plots of the differences show the consistency of both methods, as both data sets scatter ''randomly'' around the fit function. The data emerging from the BHM, however, are much more accurate than the data emerging from the standard histogram method even if much longer samples are used in the latter.

For a quantitative comparison between the two methods, the mean-square deviations of the simulation results with respect to a fit to the best data obtained by the BHM are shown as a function of the simulation time in Fig. 6. [We have performed a weighted χ^2 fit of an odd polynomial

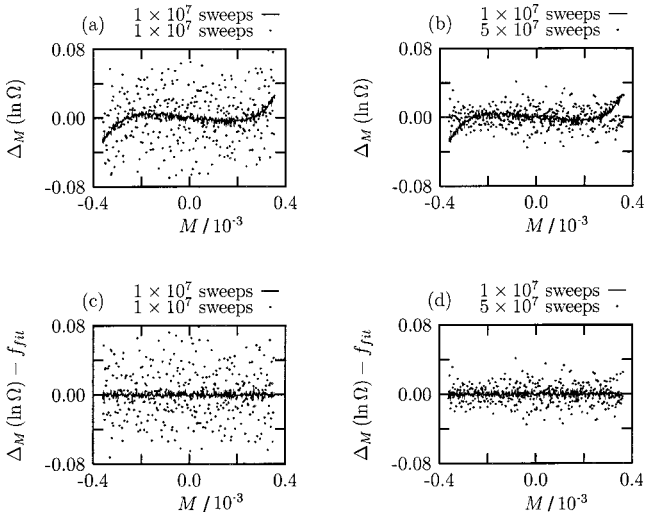

FIG. 5. In (a) and (b), differences of the logarithm of the density of states $\Delta_M(\ln\Omega)$ for a 10^3 Ising system are shown for $E/L^d=0.924$. In (a), a sample of length 1×10^7 microstates is used for the evaluation of $\Delta_M(\ln\Omega)$ according to both methods, whereas in (b), the standard histogram method with a sample length of 5×10^7 microstates is compared to the BHM with, again, sample length 1×10^7. For a better demonstration of the difference between the two methods, the same data are subtracted from a fit function in (c) and (d) (see text for the details of the fit). In all figures, the BHM data (standard histogram data) are represented by the solid lines (points).

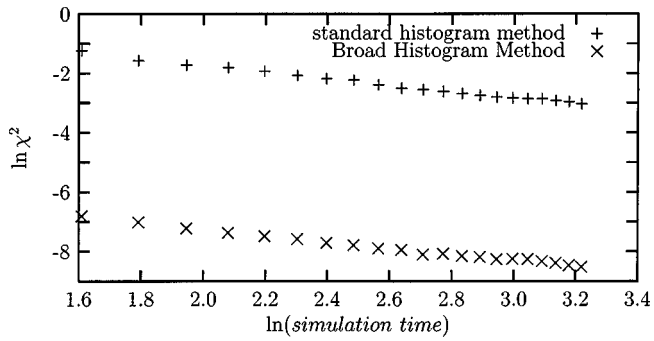

FIG. 6. In order to compare the quality of the results emerging from the standard histogram method to those emerging from the BHM for a 10^3 Ising system, the mean-square deviations of the simulation results with respect to a fit to the best data obtained by the BHM are shown as a function of the simulation time (in units of 2×10^6 lattice sweeps).

$f_{\rm fit}(M)=aM+bM^3+cM^5$ to the data obtained from a 5×10^7 sample by probing the transition observable. The errors needed for the weighted fit have been produced by a jack-knife blocking procedure using 25 data sets, each being of sample length 2×10^6]. The accuracy is improved according to a power law with an exponent of approximately -1 in both methods. Note, however, that at any given time the BHM yields results which are more accurate than the results emerging from the standard histogram method by a factor of approximately 250 in the sense of the mean-square deviation. In order to produce results of similar quality, the simulation time in the standard histogram method has to be approximately 250 times longer than in the BHM.

C. General remarks on Sec. III

(i) The two examples discussed in the preceding sections show that a simulation can be accelerated dramatically by probing the transition observable. It is not the algorithm which speeds up the simulation, but it is the particular choice of the observable which is measured during the simulation. The reason for this striking difference is indeed very simple: while every microstate, which is decided to be part of the sample, just yields one entry in a list in the standard histogram method, it might yield many transitions to neighboring states (neighboring with respect to the interaction energy and/or magnetization). Hence, the statistics of the BHM can be expected to be much better than the statistics of the standard histogram method. In fact, since the Ising systems under consideration just allow for five (seven) different interaction energy changes $[\Delta E=(\pm12),\ \pm8,\ \pm4,\ 0$ and only two magnetization changes $(\Delta M=\pm2)$ under single spin-flip operations in $d=2$ (3), the set $\mathcal{A}$ of operators chosen above can be expected to shorten the computational effort by a remarkable factor, roughly proportional to the square root of the inverse volume $L^{-d/2}$ of the system.

(ii) The change of the interaction energy under a single spin-flip operation depends on the configuration of the spins in the very neighborhood of the particular spin to be flipped. The typical configurations of neighboring spins vary with the interaction energy of the whole system. For that reason, the factor of proportionality of the efficiency gain in the sense of the χ^2 comparison introduced above can be expected to de-

pend on the mean interaction energy of the histogram, which itself depends on the simulation parameters (i.e., the stationary distribution).

(iii) The particular way of generating the sample of microstates is not important in the context of a comparison of the BHM and the standard histogram method.

IV. CONCLUSION

A Monte Carlo simulation consists of two steps. The first step is the generation of a sample of microstates. The second step is the investigation of these microstates. Conventionally, if the aim is to speed up the simulation, the first step is modified while the second remains unchanged. In a quantitative investigation, we have shown that a more extensive exploitation of the microstates of the sample, i.e., taking simulation averages of the transition observable instead of just cumulating a standard histogram, can effectively speed up the simulation by a tremendous amount.

In an extremely straightforward implementation of the BHM, a speed up is achieved which can be expected to be proportional to the square root of the volume of the system under consideration. Such a speed up seems unattainable by an improvement of the algorithm of the simulation, i.e., by modifying the first step of the simulation.

Even though the transition observable seems to be built for discrete spin systems, Muñoz and Herrmann [5] have already shown that the method can be transferred to continuous spin systems. An extension of this method to ''nonspin'' systems such as polymers might be a topic for future investigations.

ACKNOWLEDGMENTS

We would like to thank A. Hüller for valuable discussions. One of us (J. D. M.) would like to thank H. J. Herrmann for hospitality and the Deutscher Akademischer Austauschdienst for financial support.

APPENDIX A: MICROREVERSIBILITY

Let $\mathcal{A}$ be a set of operators acting on configuration space Γ_{L^d},

$$\mathcal{A}\subseteq\{A:AS\in\Gamma_{L^d}\ \ \forall\ \ S\in\Gamma_{L^d}\},\tag{29}$$

such that for all $A\in\mathcal{A}$, there exists a unique inverse operator $B=A^{-1}\in\mathcal{A}$, i.e.,

$$\forall A\in\mathcal{A}\ \ \exists!\ \ B\in\mathcal{A}:\quad BAS=S.\tag{30}$$

Then, $\mathcal{A}$ is said to show *microreversibility*. From the microreversibility of $\mathcal{A}$, it follows immediately that the number of operators $A\in\mathcal{A}$ which transform S into $\tilde{S}$ equals the number of operators $A\in\mathcal{A}$ which transform $\tilde{S}$ back into S:

$$\sum_{A\in\mathcal{A}}\delta_{AS,\tilde{S}}=\sum_{A\in\mathcal{A}}\delta_{S,A\tilde{S}}.\tag{31}$$

Using the definition of the transition observable (7), this can be shown to be equivalent to

$$\sum_{S\in\Gamma_{L^d}}\delta_{E(S),E}\delta_{M(S),M}N_{\mathcal{A}}^{i,j}(S)=\sum_{S\in\Gamma_{L^d}}\delta_{E(S),E+i\Delta E}\delta_{M(S),M+j\Delta M}N_{\mathcal{A}}^{-i,-j}(S).\tag{32}$$

That is, the number of operations which transform microstates with interaction energy E and magnetization M into microstates with $E+i\Delta E$ and $M+j\Delta M$ by use of operators $A\in\mathcal{A}$ is identical to the number of operations which transform ''backwards,'' i.e., from states with $E+i\Delta E$ and $M+j\Delta M$ to those with interaction energy E and magnetization M.

APPENDIX B: MICROCANONICAL EQUATIONS OF STATE

As mentioned in Sec. III, the differences of the logarithm of the density of states $\Delta_M(\ln\Omega)$ are related to the microcanonical magnetic equation of state. Indeed, Eq. (25) is the microcanonical magnetic equation of state in a discrete notation (appropriate for the description of finite Ising systems), which converges towards the magnetic equation of state of the infinite system,

$$-\beta h(\varepsilon,m)=\frac{\partial}{\partial m}\lim_{L\to\infty}L^{-d}\ln\Omega(L^d\varepsilon,L^d m,L^{-1}),\tag{33}$$

in the thermodynamic limit $L\to\infty$. Here, β is the inverse temperature, h is an external magnetic field, and $\varepsilon:=L^{-d}E$ and $m:=L^{-d}M$ are the intensive counterparts of E and M, respectively. The difference of the logarithm of the reduced density of states (23) converges towards $\beta(\varepsilon,\beta h)|_{h=0}$ of the infinite system for zero external field and can serve to compute zero-field properties of the system. [The inverse temperature $\beta(\varepsilon,\beta h)$ is the derivative with respect to ε of the Legendre transform of $\lim_{L\to\infty}L^{-d}\ln\Omega(L^d\varepsilon,L^d m,L^{-1})$ with respect to m. Note that (ε,β) and $(m,\beta h)$ are the pairs of conjugate variables in the entropy formalism].

Note that it is unnecessary and a rather roundabout way to convert the thus obtained data into the commonly used canonical quantities. For details on the investigation of phase transitions in a microcanonical approach and a microcanonical finite-size scaling theory, see [8].

APPENDIX C: DETAILS OF THE MONTE CARLO SIMULATION

1. Simulation of the $d=2$, $L=32$ Ising lattice

A Monte Carlo simulation of a 32^2 Ising system with periodic boundary conditions was performed. The stationary distribution of the underlying Markov process was chosen to be proportional to the Boltzmann weight $w(E(S),M(S))\propto\exp\{-\mathcal{H}(S)/T\}$ with simulation parameters $h=0$ and $T=2.269$ (see Sec. II A for the definition of the Ising Hamiltonian). We have implemented a sequential lattice update with a Metropolis-type [10] transition rate $T(S\to S')$

$=\min\{1,\hat{w}(S')/\hat{w}(S)\}$ and have sampled every L^dth configuration only. After ''equilibration'' (6.4×10^5 lattice sweeps have been discarded), several successive samples, each of length 8×10^5, were taken.

2. Simulation of the $d=3$, $L=10$ Ising lattice

A Monte Carlo simulation of a 10^3-Ising system with periodic boundary conditions was performed. The stationary distribution was chosen to be $w(E(S),M(S))\propto\{[E_0-E(S)]/N_0\}^{(N_0-2)/2}$, i.e., independent of $M(S)$ again. The simulation parameters were chosen to be $E_0=1586$ and $N_0=1000$ (for a detailed discussion and interpretation of this stationary distribution, see [11]). The way of updating the lattice configurations is the same as for the simulation of the 32^2-Ising system (see Appendix C). After ''equilibration'' (2×10^6 lattice sweeps have been discarded), several successive samples, each of length 2×10^6, were taken.

[1] Z. W. Salsburg, J. D. Jacobson, W. Fickett, and W. W. Wood, J. Chem. Phys. **30**, 65 (1959).

[2] A. M. Ferrenberg and R. H. Swendsen, Phys. Rev. Lett. **61**, 2635 (1988); R. H. Swendsen, Physica A **194**, 53 (1993).

[3] P. M. C. de Oliveira, T. J. P. Penna, and H. J. Herrmann, Braz. J. Phys. **26**, 677 (1996); Eur. Phys. J. B **1**, 205 (1998); P. M. C. de Oliveira, *ibid.* **6**, 111 (1998).

[4] A. R. Lima, P. M. C. de Oliveira, and T. J. P. Penna, e-print cond-mat/9912152 (unpublished).

[5] J. D. Muñoz and H. J. Herrmann, J. Mod. Phys. C **10**, 95 (1999); in *Computer Simulation Studies in Condensed Matter Physics XII*, edited by D. P. Landau, S. P. Lewis, and H.-B. Schüttler (Springer Verlag, Heidelberg, 1999).

[6] M. Deserno, Phys. Rev. E **56**, 5204 (1997).

[7] G. R. Smith and A. D. Bruce, J. Phys. A **28**, 6623 (1995); R. H. Swendsen and S.-T. Li (unpublished); J.-S. Wang, T. K. Tay, and R. H. Swendsen, Phys. Rev. Lett. **82**, 476 (1999).

[8] M. Kastner, M. Promberger, and A. Hüller, J. Stat. Phys. **99**, 1251 (2000); M. Kastner, *Critical Phenomena in the Entropy Formalism and Microcanonical Finite-Size Scaling* (Shaker-Verlag, Aachen, 2000).

[9] P. D. Beale, Phys. Rev. Lett. **76**, 78 (1996).

[10] N. Metropolis *et al.*, J. Chem. Phys. **21**, 1087 (1953).

[11] A. Hüller and R. W. Gerling, Z. Phys. B. **90**, 207 (1993).